Optimization of structural and technological parameters of the field effect Hall sensor

Volchek V., Lovshenko I.,
Stempitsky V., Dao Dinh Ha
Establishment of Education “Belarusian State University of Informatics and Radioelectronics” (BSUIR)
Minsk, Belarus
vstem@bsuir.by

Belous A., Saladukha V.
Joint Stock Company “Integral”
Minsk, Belarus
office@bms.by

***Abstract*— The results of optimization of magnetically sensitive element Field Hall sensor based on the MIS structure formed on a "silicon-on-insulator" (SOI LSF) parameters was presented. Main characteristics of device structure were defined using the results of Silvaco software simulation.**

Keywords—sensitive element, Field Hall sensor; optimization, SOI

I. Introduction

The effective functioning of various monitoring and control systems often requires the use of magnetic field sensors. The sensing element in devices of this type is a transducer that transforms an electric signal according to the intensity of an applied magnetic field, for example, a Hall sensor (HS) [1, 2]. Standard Hall sensors are passive recorders of external influences. Hall sensors based on SOI technology also allow registering of a magnetic signal, controlling the magnitude of an output signal, and measuring in digital and analog modulation modes [3].

II. Structure

The structure of the investigated field effect Hall sensor based on SOI technology (SOI FEHS) is illustrated in Figure 1. A 400 nm buried oxide layer (2) was created by a known technique [4] on a silicon substrate (1) of n-type conductivity with a concentration of $5 \cdot 10^{16}$ cm^{-3}. The buried oxide separates a 200 nm device layer (3), also called an active area, from the bulk silicon. In the active area a Hall cross was made by two strips measuring L = 25 µm long and W = 10 µm wide. To form ohmic contacts (4) to both the current (5) and the Hall (9) electrodes the sections adjacent to the strip ends were doped by phosphorus with a concentration up to 10^{21} cm^{-3}. The cross surface was covered by a 100nm pyrolitic oxide film (7) above which was deposited an aluminum film (6). This construction is a top gate. For a bottom gate (8) the silicon substrate with a deposited aluminum film was used. The useful signal is taken from the Hall electrodes (9).

Depending on the polarity and the value of gate-to-source voltage, the depth of the layer where the Hall effect manifests itself can vary from the thickness of the silicon layer to nearly zero. It is important to note that the threshold sensitivity of SOI FEHS’s exceeds by an order of magnitude that of silicon HS’s [4]. The buried oxide reduces the substrate leakage currents by several orders of magnitude resulting in an increase in operating temperature in comparison with standard HS’s (from -40 to 125 °C) [3].

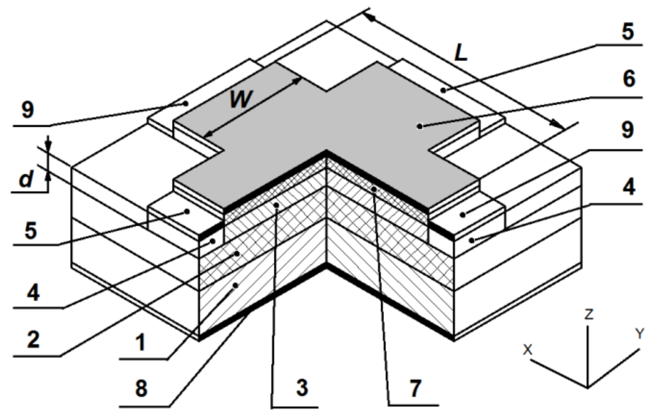

Fig. 1. Structure of the field effect Hall sensor based on silicon-on-insulator technology.

Hall voltage is dependent on the active area thickness d, the geometrical factor G, the Hall coefficient Rh, the induction of the applied magnetic field B, and the intensity of the current I flowing between the current contacts as follows: $U_h = G \cdot R_h \cdot I \cdot B / d$.

The geometrical factor G is dependent on the length-to-width ratio L / W. The finite length correction factor is relatively small. When the ratio L / W = 2 the geometrical factor G equals 0.95, and when the ratio L / W = 3 the correction factor is only 1 %. Therefore, there is no point in increasing the length-to-width ratio and in practice it is usually in the range of 2 to 3 [4].

III. Results

The simulations of the structure and the electrical behavior were performed using Atlas software from Silvaco [6]. For the SOI FEHS under review the influence of structural and technological parameters on the device sensitivity was studied.

A comparative analysis of the simulation results showed that the proportional decrease in the length and width of the structure from the values of L = 50 µm, W = 20 µm to L = 25 µm, W = 10 µm leads to the increase in the absolute sensitivity by 43 % (from 70 to 100 mV / T), the current sensitivity by 47 % (from 180 to 265 V / A · T). The voltage sensitivity remains constant, equal to 30 mV / V · T. The decrease in the gate dielectric thickness to 0.1 µm brings to the increase in the absolute sensitivity by 48 % (from 135 to 200 mV / T), the current sensitivity by 45 % (from 180 to 265 V / A · T). The voltage sensitivity decreases by 17 % (from 30 to 25 mV / V · T).

Figure 2 shows output characteristic plots of the Hall voltage U_h as a function of an applied magnetic field B. The output characteristics of the SOI FEHS are linearly proportional to the magnetic field intensity in the whole dynamic range as well. As is evident from the figure, the Hall voltage is nearly independent of the structure dimensions while maintaining the L / W = 2 ratio constant.

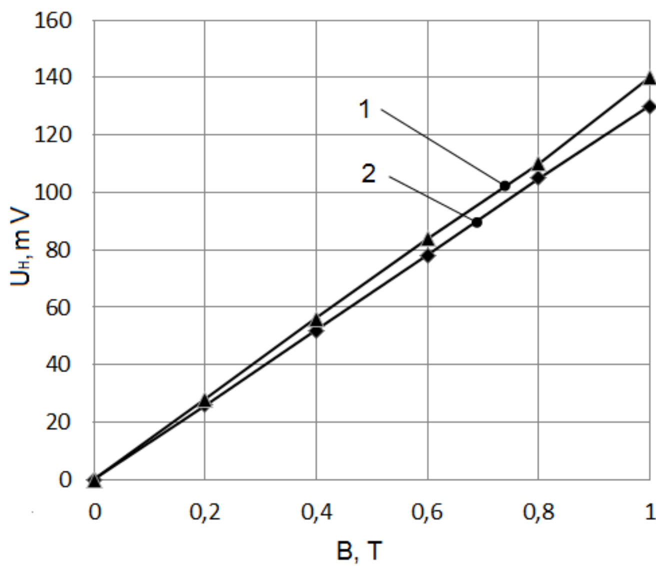

Fig. 2. Hall voltage U_h versus magnetic induction B for the following structure dimensions: L = 25 µm, W = 10 µm (1) and L = 50 µm, W = 20 µm (2).

Temperature dependencies of the Hall electromotive force (Hall EMF) in reduced units, i.e., normalized by the EMF value corresponding to the temperature of 250 K, are given in Figure 3. These dependencies were obtained for different structure dimensions with the following operating point parameters: supply voltage = 5.0 V and gate voltage = 2.5 V. The results display that the Hall voltage halves when the temperature rises to 400 K. At higher temperatures the dependence slightly weakens. Thus, the Hall voltage alters only by 10 % (from 100 to 75 mV) as the temperature grows from 400 to 450 K.

Simulations of the SOI FEHS structures with various active area materials were also carried out. Based on [6-7], for the simulations as the active area materials were utilized silicon (Si), germanium (Ge), gallium arsenide (GaAs), and indium antimonide (InSb).

Figure 4 shows plots of the SOI FEHS sensitivity S as a function of an applied magnetic field B.

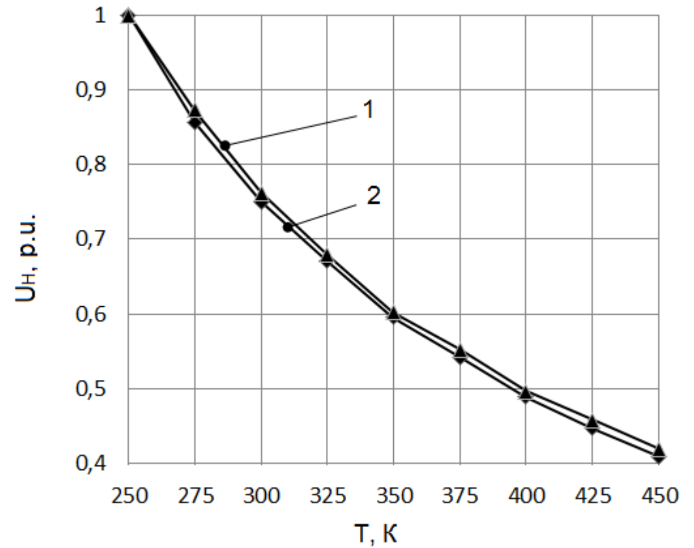

Fig. 3. Hall voltage U_h in reduced units versus temperature T for the following structure dimensions: L = 25 µm, W = 10 µm (1) and L = 50 µm, W = 20 µm (2).

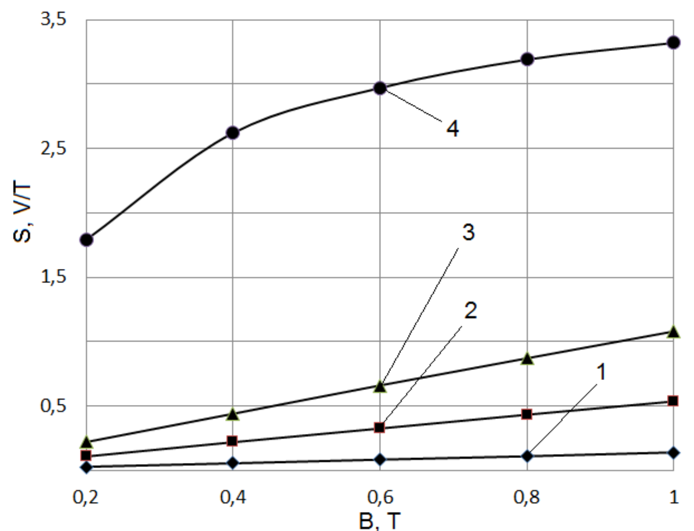

Fig. 4. Sensitivity S versus magnetic induction B for the structures with the various active area materials: Si (1); Ge (2); GaAs (3); InSb (4).

As follows from the plots, at B = 0.6 T the sensitivity of the SOI FEHS with the indium antimonide active area is around six times larger than that of the other structures with the silicon, germanium, or gallium arsenide active areas. The indium antimonide SOI FEHS structure has a non-linear sensitivity dependence on magnetic induction, as opposed to the other structures. The increase in the magnetic induction from 0.2 T to 0.4 T causes a sensitivity change of 44 % (from 1.8 to 2.6 V / T). The further increase in the magnetic induction to 0.6 T leads to a sensitivity change of 15 % (from 2.6 to 3.0 V / T). This fact complicates the data processing scheme in SOI FEHS's.

Temperature dependencies of the SOI FEHS sensitivity for the various active area materials are presented in Figure 5.

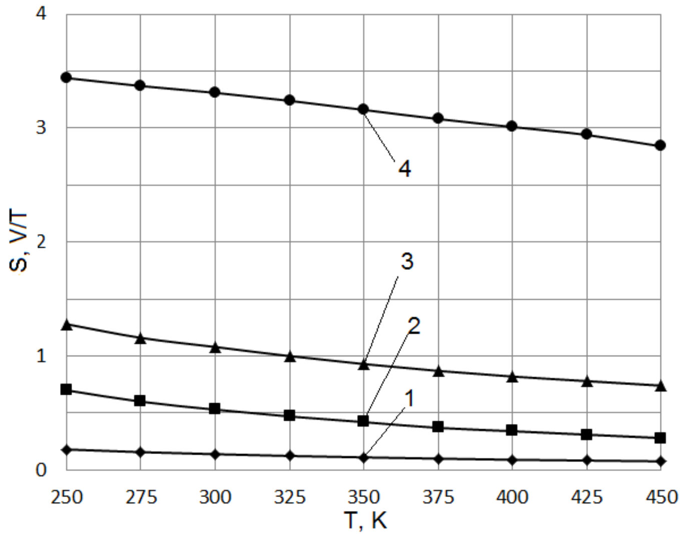

Fig. 5. Sensitivity S versus temperature T for the structures with the various active area materials: Si (1); Ge (2); GaAs (3); InSb (4).

As is obvious from the figure, applying indium antimonide as an active area material allows decreasing the nonlinearity of the temperature dependence. Thus, while the Si SOI FEHS sensitivity halves at 400 K and the decreases for the Ge and GaAs sensors are 50 % (from 0.7 V / T at 250 K to 0.35 V / T at 400 K) and 33 % (from 1.2 V / T at 250 K to 0.8 V / T at 400 K) correspondingly, the InSb SOI FEHS sensitivity drops by 14 % (from 3.5 V / T at 250 K to 3.0 V / T at 400 K).

Figure 6 shows plots of the SOI FEHS sensitivity S as a function of the voltage on the current electrodes Vd for the various active area materials.

As follows from the figure, the dependencies are linear at the voltage range of 1 to 5 V. The voltage on the current electrodes influences most the sensitivity of the InSb SOI FEHS. The increase in the voltage by 1 V causes the increase in the sensitivity more than by 60 % (from 1.1 V / T at 2 V to 1.85 V / T at 3 V). For the Si, Ge and GaAs structures this change is 13 %, 20 % and 40 %, respectively.

Thus, owing to the presence of the vertical two-gate control system in the SOI FEHS there exists the capability for modulating the useful signal (Hall EMF) by the gate voltage that is carried out by changing the sensitivity of the SOI FEHS. The analysis of the structural and technological parameters influence on the HS sensitivity showed that decreasing by half linear device dimensions while keeping the length-to-width ratio L / W constant and equal 2 increases values of the absolute sensitivity for the structures with the thickness of the active area d = 0.2 μm by 30 % (from 70 to 100 mV / T), and the thickness d = 0.1 μm by 48 % (from 135 to 200 mV / T). The output characteristic is linear. With the ratio L / W being kept constant and equal 2, device dimensions have a weak influence on both the temperature dependence of the SOI FEHS and the output characteristic. The SOI FEHS continues to function well at the range of higher temperatures inaccessible to his bulk silicon counterparts. Indium antimonide can be considered as a perspective material for SOI FEHS.

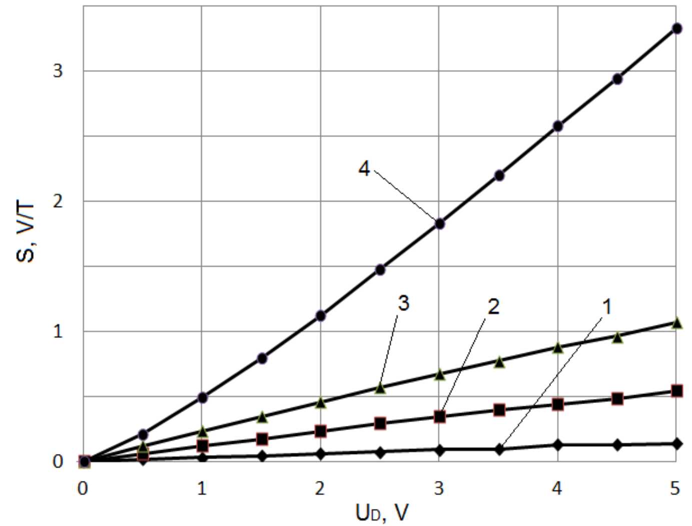

Fig. 6. Sensitivity S versus voltage on the current electrodes UD for the structures with the various active area materials: Si (1); Ge (2); GaAs(3); InSb (4).

Acknowledgment

This work was supported by the grant 1.1.16 of Belarusian National Scientific Research Program “Electronics and Photonics”

References

[1] Dolgiy L., I. Lovshenko, V. Nelayev, I. Shelibak, S. Shvedov, A. Turtsevich Technology and Device Design and Optimization for the MOSFET Hall Sensor on SOI Structure // Proc. of the Int. Conf. MIXED Design of Integrated citcuits and systems 2012. – Warszawa: Remigraf, 2012. – P. 398 -400.

[2] R. S. Popovic. Hall Effect Devices / Institute of Physics Publishing. - 2004.

[3] E. Ramsden. Hall-Effect Sensors – Theory and Applications / Elsevier, 2006.

[4] M. Paun, F. Udrea. SOI Hall cells design selection using three – dimensional physical simulations / Journal of Magnetism and Magnetic Materials. - № 372. – 2014. – pp. 141–146

[5] http://www.silvaco.com/

[6] H. P. Baltes, S. P Radivoje. Integrated Semiconductor Magnetic Field Sensors / Proceedings of the IEEE. - vol. 74. - № 8. – 1986. - pp. 1107-1132.

[7] A. Sandhu, A. Okamoto, I. Shibasaki, A. Oral, Nano and micro Hall-effect sensors for room-temperature scanning hall probe microscopy / Microelectronic Engineering . - № 73–74. – 2004. - pp. 524–528.